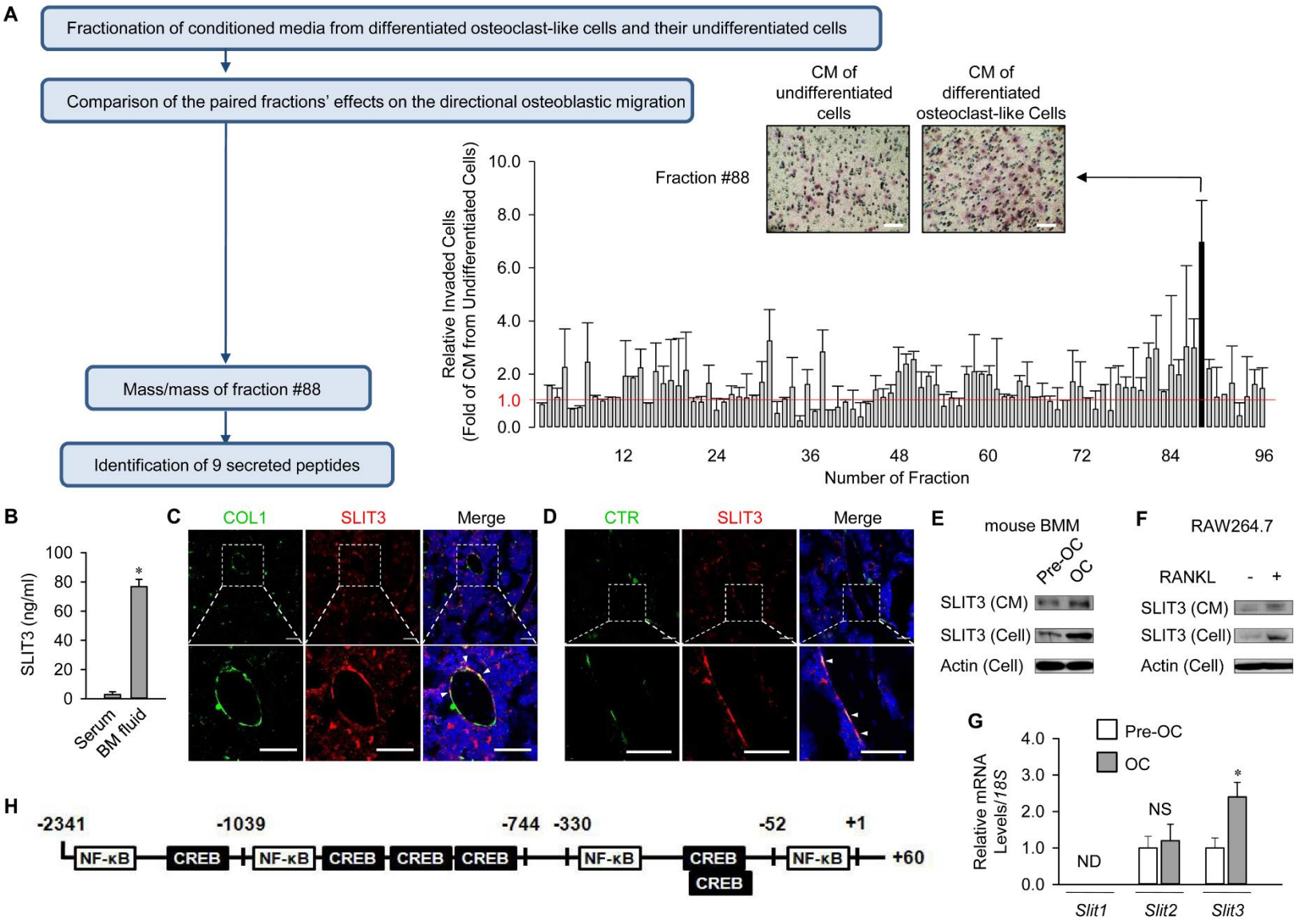
A
Fractionation of conditioned media from differentiated osteoclast-like cells and their undifferentiated cells
Comparison of the paired fractions' effects on the directional osteoblastic migration
Mass/mass of fraction #88
Identification of 9 secreted peptides
CM of undifferentiated cells
CM of differentiated osteoclast-like Cells
Fraction #88
Relative Invaded Cells (Fold of CM from Undifferentiated Cells)
Number of Fraction
B
SLIT3 (ng/ml)
Serum
BM fluid
C
COL1
SLIT3
Merge
D
CTR
SLIT3
Merge
E
mouse BMM
Pre-OC
OC
SLIT3 (CM)
SLIT3 (Cell)
Actin (Cell)
F
RAW264.7
RANKL
SLIT3 (CM)
SLIT3 (Cell)
Actin (Cell)
G
Pre-OC
OC
Relative mRNA Levels/18S
ND
NS
Slit1
Slit2
Slit3
H
-2341
-1039
-744
-330
-52
+1
+60
NF-κB
CREB

Supplemental Figure 1. Expression of SLIT3 in Pre-osteoclasts and Differentiated Osteoclasts

(A) A fractionated secretomic approach to the identification of osteoclast-derived factors that stimulate directional migration of osteoblasts. Osteoclast-like cells were generated from murine macrophage RAW264.7 cells treated with 15 ng/ml RANKL. Primary mouse cell cultures were not used to avoid contamination with other cells. The conditioned media (CM) of RAW264.7 cells cultured in the presence or absence of RANKL were collected and separated into 96 fractions. Each paired fraction was then used to treat murine pre-osteoblast MC3T3-E1 cells. Scale bar, 100 μm. Liquid chromatography-mass spectrometry/mass spectrometry (LC-MS/MS) was performed on fraction pair #88, which showed the largest difference in the ability to stimulate the directional migration of osteoblasts. The MASCOT database was used to identify nine secretory proteins that were elevated in the CM of osteoclast-like cells. **(B)** ELISA experiment to determine the SLIT3 concentrations in the serum and bone marrow fluid of 5-week-old C57BL/6 male mice (n = 3). The mean values from duplicate samples are shown. **(C and D)** IHC staining to assay SLIT3 expression in the osteoblasts (C) and osteoclasts (D) of bone tissues. Immunofluorescence images of collagen type 1 (COL1, green) or calcitonin receptor (CTR, green) and SLIT3 (red) in the femurs of 12-week-old male C57BL/6 mice (n = 3) are shown. SLIT3 was detected around both cell types at the bone surface (white, arrowheads). Representative enlarged images from inset in top panels (bottom panels); ×5 magnifications. Scale bar, 50 μm. **(E)** Western blot analysis of SLIT3 in the CM and cell lysates (Cell) from pre-osteoclasts (pre-OC) and differentiated osteoclasts (OC). Pre-OCs and OCs were generated from mouse bone marrow macrophages (BMMs) treated with 15 ng/ml M-CSF in the presence or absence of 15 ng/ml RANKL for 3 days, respectively. CM samples were collected during the subsequent 24 h period under the same conditions. **(F)** Western blot

analysis of SLIT3 in the CM and cell lysates of RAW264.7 cells incubated in the presence or absence of 15 ng/ml RANKL for 3 days. CM samples were collected during the subsequent 24 h period under the same conditions. **(G)** Quantitative RT-PCR analysis of *Slit* family members in pre-OCs and OCs differentiated from mouse BMMs treated with 15 ng/ml M-CSF in the presence or absence of 15 ng/ml RANKL for 3 days, respectively. *18S* RNA was used as the loading control. **(H)** Putative binding sites for NF-κB and CREB in the promoter region of *Slit3*. Error bars denote the mean ± SEM. In vitro experiments were performed 3 times independently. $^{*}p < 0.05$ *vs*. control or pre-OCs using the Mann–Whitney U-test. ND, not detected. NS, not significant.

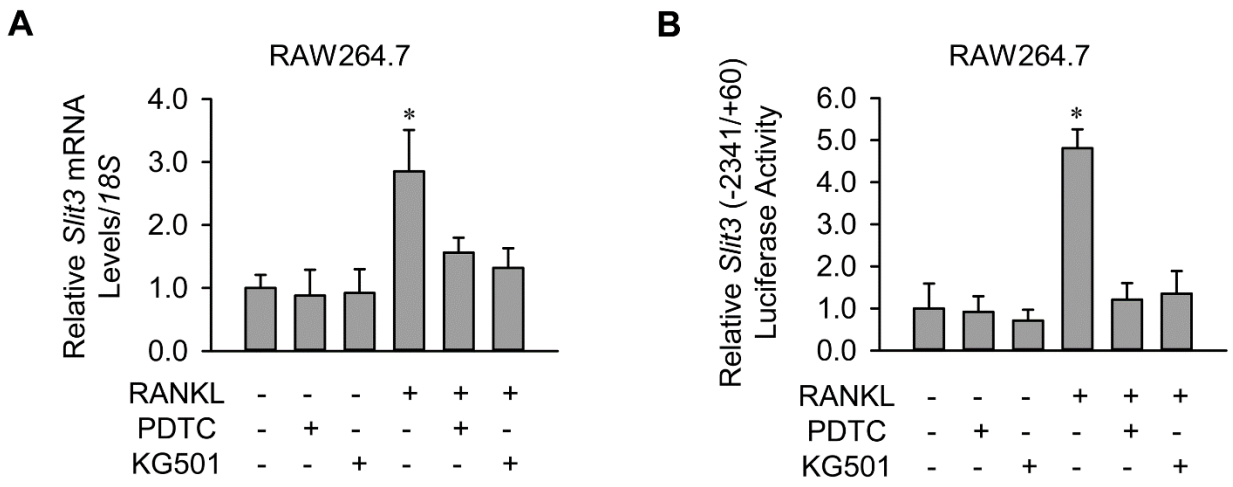

Supplemental Figure 2. Crucial Role of NFκB p50 and CREB in RANKL-stimulated SLIT3 Expression in Raw264.7 Cells

(A and B) Quantitative RT-PCR (A) and luciferase assay (B) analysis of RAW264.7 cells performed before and after pretreatment with inhibitors of NF-kB p50 and CREB (PDTC and KG501, respectively). $^{*}p < 0.05$ *vs*. untreated control using the Kruskal–Wallis test followed by Bonferroni correction.

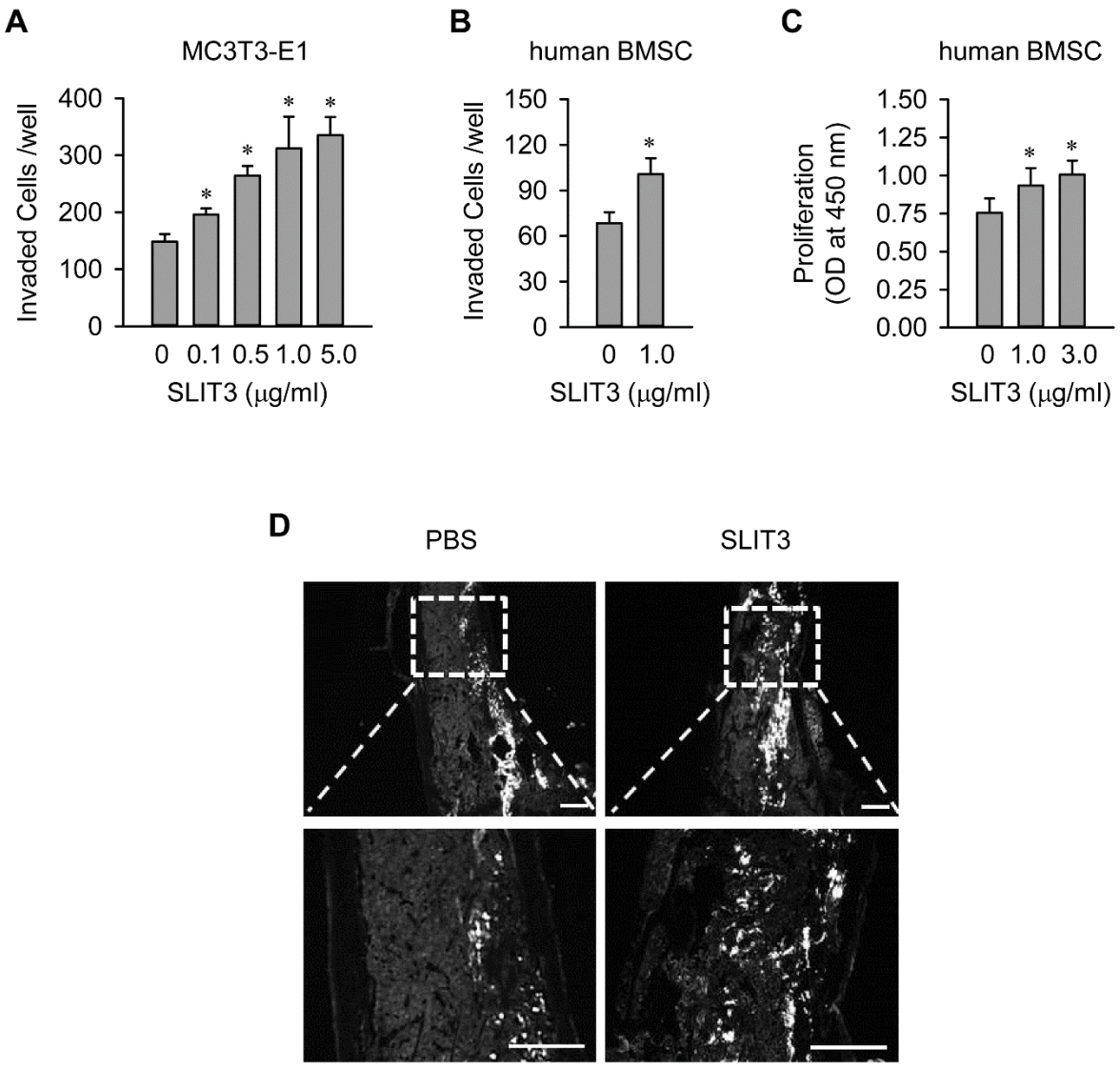

Supplemental Figure 3. Effect of SLIT3 on the Directional Migration and Proliferation of Osteoblast Lineages

(A and B) Directional migration of MC3T3-E1 cells (A) and human bone marrow stromal cells (BMSCs) (B) in the presence of SLIT3 for 24 h, analyzed using a Boyden chamber system. The invaded cell numbers were counted. **(C)** Proliferation of human BMSCs after exposure to SLIT3 for 48 h measured using a BrdU incorporation assay. **(D)** Representative image of intra-bone marrow mobilization of green fluorescent protein (GFP)-labeled MC3T3-E1 cells. PBS (control,

left tibia) or 300 μg/kg SLIT3 (right tibia) were injected into the bone marrow cavity for 3 days. Representative enlarged images from inset in top panels (bottom panels); ×3 magnifications. Scale bar, 500 μm. Error bars denote the mean ± SEM. In vitro experiments were performed 3–5 times independently. $^{*}p < 0.05$ *vs*. untreated control using the Mann–Whitney U-test or Kruskal–Wallis test followed by Bonferroni correction.

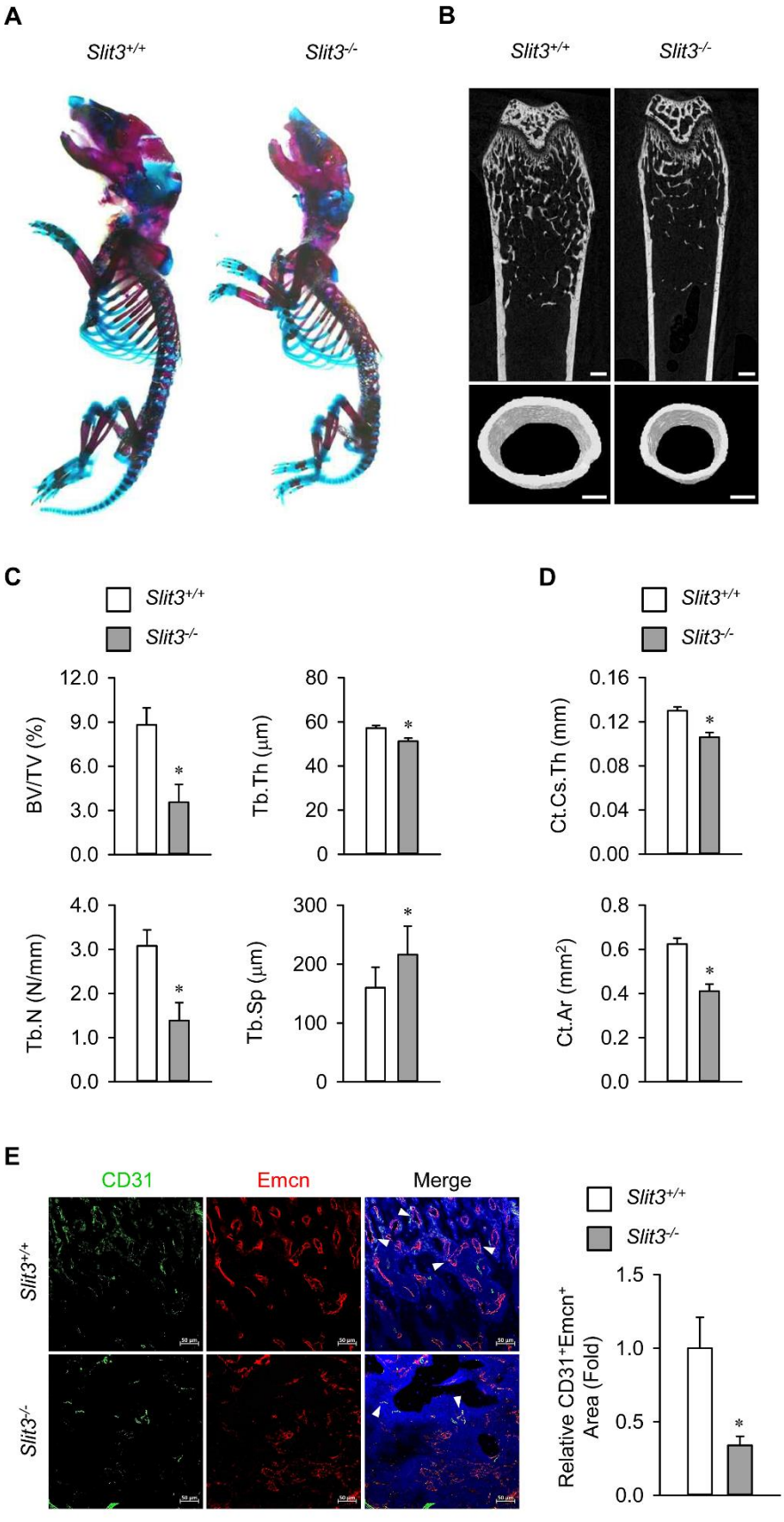
A
Slit3+/+
Slit3-/-
B
Slit3+/+
Slit3-/-
C
Slit3+/+
Slit3-/-
BV/TV (%)
12.0
9.0
6.0
3.0
0.0
Tb.Th (μm)
80
60
40
20
0
Tb.N (N/mm)
4.0
3.0
2.0
1.0
0.0
Tb.Sp (μm)
300
200
100
0
D
Slit3+/+
Slit3-/-
Ct.Cs.Th (mm)
0.16
0.12
0.08
0.04
0.00
Ct.Ar (mm2)
0.8
0.6
0.4
0.2
0.0
E
CD31
Emcn
Merge
Slit3+/+
Slit3-/-
Slit3+/+
Slit3-/-
Relative CD31+Emcn+ Area (Fold)
1.5
1.0
0.5
0.0

Supplemental Figure 4. Osteopenic Phenotypes in *Slit3*$^{-/-}$ Mice

(A) Cartilage and bones of whole newborn male mice visualized by Alcian Blue and Alizarin Red staining, respectively (n = 4 per group). **(B)** Microcomputed tomography analyses of the femurs of 7-week-old male *Slit3*$^{-/-}$ mice and wild-type littermates (n = 4–5 per group). Scale bar, 500 μm. **(C and D)** Assessment of trabecular and cortical bone parameters. Bone volume/tissue volume (BV/TV), trabecular thickness (Tb.Th), trabecular number (Tb.N), trabecular separation (Tb.Sp), cortical thickness (Ct.Cs.Th), and cortical bone area (Ct.Ar). **(E)** Effects of SLIT3 on the formation of type H vessels ($CD31^+Emcn^+$ endothelium). Immunofluorescence (IF) images of CD31 (green) and endomucin (Emcn, red) in the femurs of 8-week-old female *Slit3*$^{-/-}$ mice and wild-type littermates (n = 3–4 per group). $CD31^+Emcn^+$ vessels (white, arrowheads) were found to be decreased in femurs from *Slit3*$^{-/-}$ mice. The $CD31^+Emcn^+$ area in the femurs was quantified. Scale bar, 50 μm. Error bars denote the mean ± SEM. $^*p < 0.05$ *vs*. wild-type mice using the Mann–Whitney U-test.

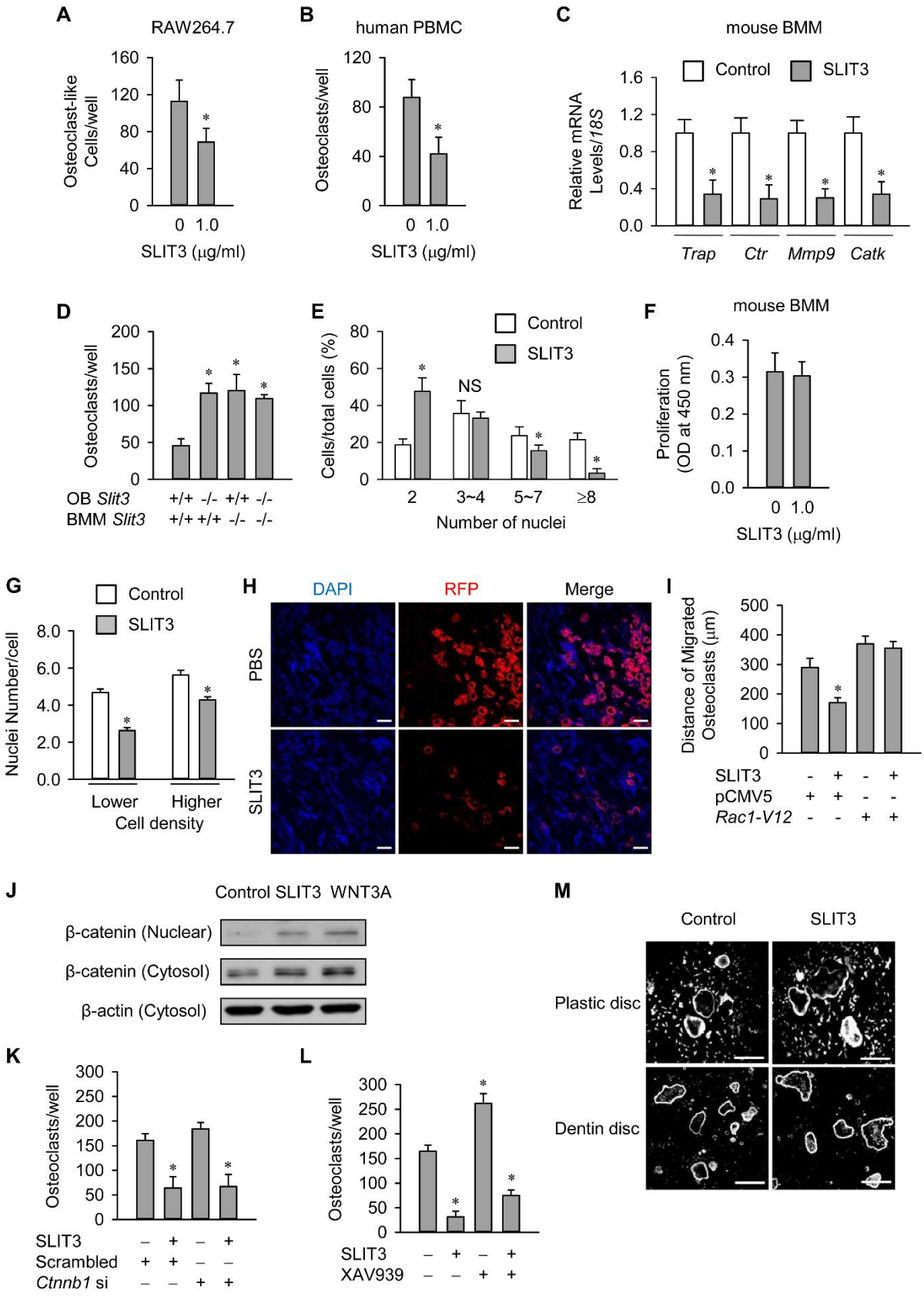
A
RAW264.7
Osteoclast-like Cells/well
160
120
80
40
0
0 1.0
SLIT3 (μg/ml)
B
human PBMC
Osteoclasts/well
120
80
40
0
0 1.0
SLIT3 (μg/ml)
C
mouse BMM
Control
SLIT3
Relative mRNA Levels/18S
1.6
1.2
0.8
0.4
0.0
Trap
Ctr
Mmp9
Catk
D
Osteoclasts/well
200
150
100
50
0
OB Slit3 +/+ -/- +/+ -/-
BMM Slit3 +/+ +/+ -/- -/-
E
Control
SLIT3
Cells/total cells (%)
80
60
40
20
0
NS
2
3~4
5~7
≥8
Number of nuclei
F
mouse BMM
Proliferation (OD at 450 nm)
0.4
0.3
0.2
0.1
0.0
0 1.0
SLIT3 (μg/ml)
G
Control
SLIT3
Nuclei Number/cell
8.0
6.0
4.0
2.0
0.0
Lower
Higher
Cell density
H
DAPI
RFP
Merge
PBS
SLIT3
I
Distance of Migrated Osteoclasts (μm)
500
400
300
200
100
0
SLIT3 - + - +
pCMV5 + + - -
Rac1-V12 - - + +
J
Control SLIT3 WNT3A
β-catenin (Nuclear)
β-catenin (Cytosol)
β-actin (Cytosol)
K
Osteoclasts/well
300
250
200
150
100
50
0
SLIT3 – + – +
Scrambled + + – –
Ctnnb1 si – – + +
L
Osteoclasts/well
300
250
200
150
100
50
0
SLIT3 – + – +
XAV939 – – + +
M
Control
SLIT3
Plastic disc
Dentin disc

Supplemental Figure 5. Effect of SLIT3 on Osteoclast Differentiation

(A and B) Tartrate-resistant acid phosphatase (TRAP) staining of RAW264.7 cells exposed to 15 ng/ml RANKL (A) and human peripheral blood mononuclear cells (PBMCs) exposed to 25 ng/ml M-CSF and 30 ng/ml RANKL (B) in the presence or absence of SLIT3 for 4–6 days. TRAP-positive cells with more than three nuclei were counted. **(C)** Quantitative RT-PCR expression analysis of osteoclast differentiation markers (*Trap, calcitonin receptor* [*Ctr*], *matrix metallopeptidase 9* [*Mmp9*], *and cathepsin K* [*Catk*]) in mouse bone marrow macrophages (BMMs) exposed to 15 ng/ml M-CSF and 15 ng/ml RANKL in the presence or absence of 1.0 μg/ml SLIT3 for 4 days. **(D)** TRAP staining of osteoclasts, co-cultured with osteoblasts. Mouse BMMs and osteoblasts were obtained from *Slit3*$^{-/-}$ mice and their littermate controls, and were co-cultured with 50 μg/ml ascorbic acid and 10 mM β-glycerophosphate for 10–14 days. TRAP-positive cells with more than three nuclei were counted. **(E)** TRAP staining of mouse BMMs treated with 15 ng/ml M-CSF and 15 ng/ml RANKL for 2–3 days. Cells with more than two nuclei were analyzed. The percentages of cells with the indicated numbers of nuclei were counted. **(F)** Proliferation of mouse BMMs exposed to M-CSF in the presence or absence of SLIT3 for 48 h using a BrdU incorporation assay. **(G)** TRAP staining of mouse BMMs in 96-well plates at a lower (0.4×10^4 cells/well) or higher (10×10^4 cells/well) cell density treated with 15 ng/ml M-CSF and 15 ng/ml RANKL for 2–3 days. The number of nuclei per cell was counted. **(H)** Representative image of the intra-bone marrow mobilization of red fluorescent protein (RFP)-labeled BMMs. PBS (control, left tibia) and 300 μg/kg SLIT3 (right tibia) were injected into the bone marrow cavity for 3 days. Scale bar, 500 μm. **(I)** Osteoclast migration on dentine discs in the presence or absence of 1.0 μg/ml SLIT3 after transfection of pCMV5 (empty vector) or *Rac1-V12* (*Rac1* overexpression vector). Osteoclasts were cultured on dentin discs with 30 ng/ml M-CSF and 30 ng/ml RANKL for 2 days. The length

of the pits (cell migration length) was evaluated using the Image-Pro Plus program. **(J)** Western blotting analysis of β-catenin in BMMs. Mouse BMMs were cultured with 15 ng/ml M-CSF in the presence or absence of 1.0 μg/ml SLIT3 for 4 h. Wnt3a CM was used as a positive control. Cell fractionation was performed to obtain nuclear and cytosolic proteins. **(K and L)** TRAP staining of mouse BMMs exposed to 15 ng/ml M-CSF and 15 ng/ml RANKL in the presence or absence of 1.0 μg/ml SLIT3 for 4 days after the transfection of β-catenin siRNA (*Ctnnb1* si) or a scrambled control (K). A chemical inhibitor of Wnt/β-catenin pathway (XAV939) was used to pre-treat the cells in the place of β-catenin siRNA (L). TRAP-positive cells with more than three nuclei were counted. **(M)** Osteoclast actin ring formation induced by SLIT3. Mouse BMMs were treated with 15 ng/ml M-CSF and 15 ng/ml RANKL in the presence or absence of 1.0 mg/ml SLIT3 in plastic or dentin discs. The cells were then stained with FITC-phalloidin. Scale bar, 100 μm. Error bars denote the mean ± SEM. In vitro experiments were performed at 3–4 times independently. $^{*}p < 0.05$ *vs*. untreated, empty vector-transfected, or scrambled siRNA-transfected cells using the Mann–Whitney U-test or Kruskal–Wallis test followed by Bonferroni correction.

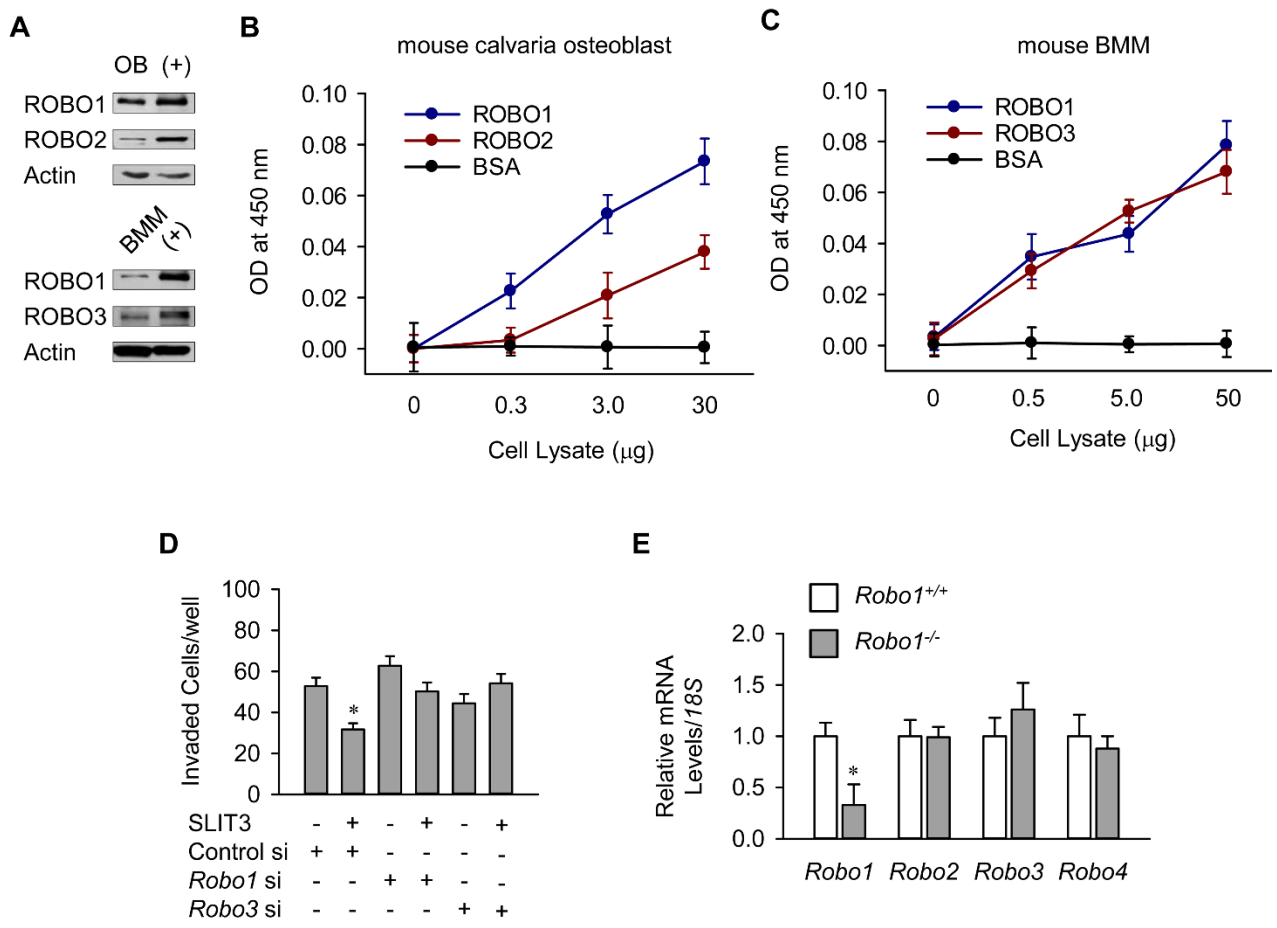

Supplemental Figure 6. SLIT3 Receptors in Osteoblasts and Bone Marrow Macrophages

(A) Western blotting analysis of ROBO1 and ROBO2 in mouse calvaria osteoblasts (OB), and of ROBO1 and ROBO3 in mouse bone marrow macrophages (BMM). Mouse brain was used as a positive control (+). **(B)** Interaction of SLIT3 with ROBO1 and ROBO2 in mouse calvaria OBs in a binding ELISA assay. Various amounts of mouse calvaria OBs lysates were incubated for 2 h into 10 μg/ml SLIT3- or BSA-coated wells, followed by determining the amounts of ROBO1 and ROBO2 by ELISA. **(C)** Interaction of SLIT3 with ROBO1 and ROBO3 in mouse BMMs in a binding ELISA assay. Various amounts of mouse BMM lysates were incubated into SLIT3- or BSA-coated wells, followed by a determination of the amounts of ROBO1 and ROBO3 by ELISA. **(D)** Directional migration of mouse BMMs in the presence of 1.0 μg/ml SLIT3 for 24 h after

transfection with *Robo1* siRNA or *Robo3* siRNA. The extent of the migration was assessed using a Boyden chamber system by counting the invaded cell numbers. **(E)** Quantitative RT-PCR analysis of *Robo* expression in the femurs, including the bone marrow, of 7-week-old *Robo1*$^{-/-}$ male mice and wild-type littermates (n = 4–5 per group). Error bars denote the mean ± SEM. In vitro experiments were performed at least 3 times independently. $^{*}p < 0.05$ *vs*. untreated control or wild-type mice using the Mann–Whitney U-test or Kruskal–Wallis test followed by Bonferroni correction.

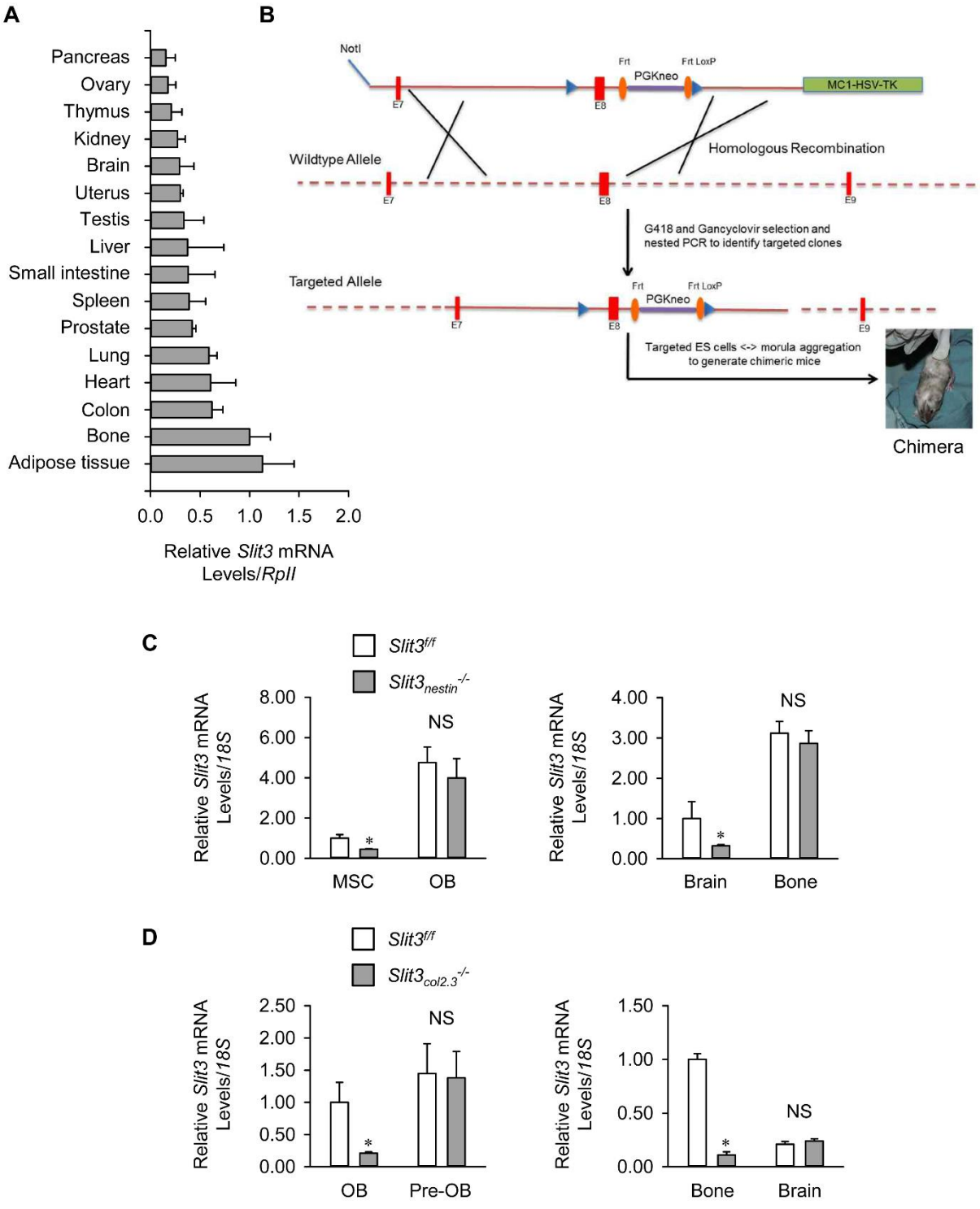

Supplemental Figure 7. Generation of Neuron- and Osteoblast-specific *Slit3*-deficient Mice

(A) *Slit3* expression in various organs of 16-week-old male or female C57BL/6 mice (n = 3 in each

organ) measured by quantitative RT-PCR. *RpII* RNA was used as the loading control. **(B)** Design of the floxed allele of *Slit3*. **(C)** Quantitative RT-PCR analysis of *Slit3* expression in mesenchymal stem cells (MSC) and osteoblasts (OB) obtained from 6-week-old male $Slit3_{nestin}^{-/-}$ and their $Slit3^{f/f}$ littermates (n = 3 per group). *Slit3* expression in the brains of 16-week-old male mice was also tested in comparison with the femurs. **(D)** Quantitative RT-PCR analysis of *Slit3* expression in osteoblasts, their precursors (pre-OB), the femurs, and the brains of $Slit3_{col2.3}^{-/-}$ and their $Slit3^{f/f}$ littermates (n = 3 per group). Error bars denote the mean ± SEM. $^{*}p < 0.05$ *vs*. littermate control using the Mann–Whitney U-test. NS, not significant.

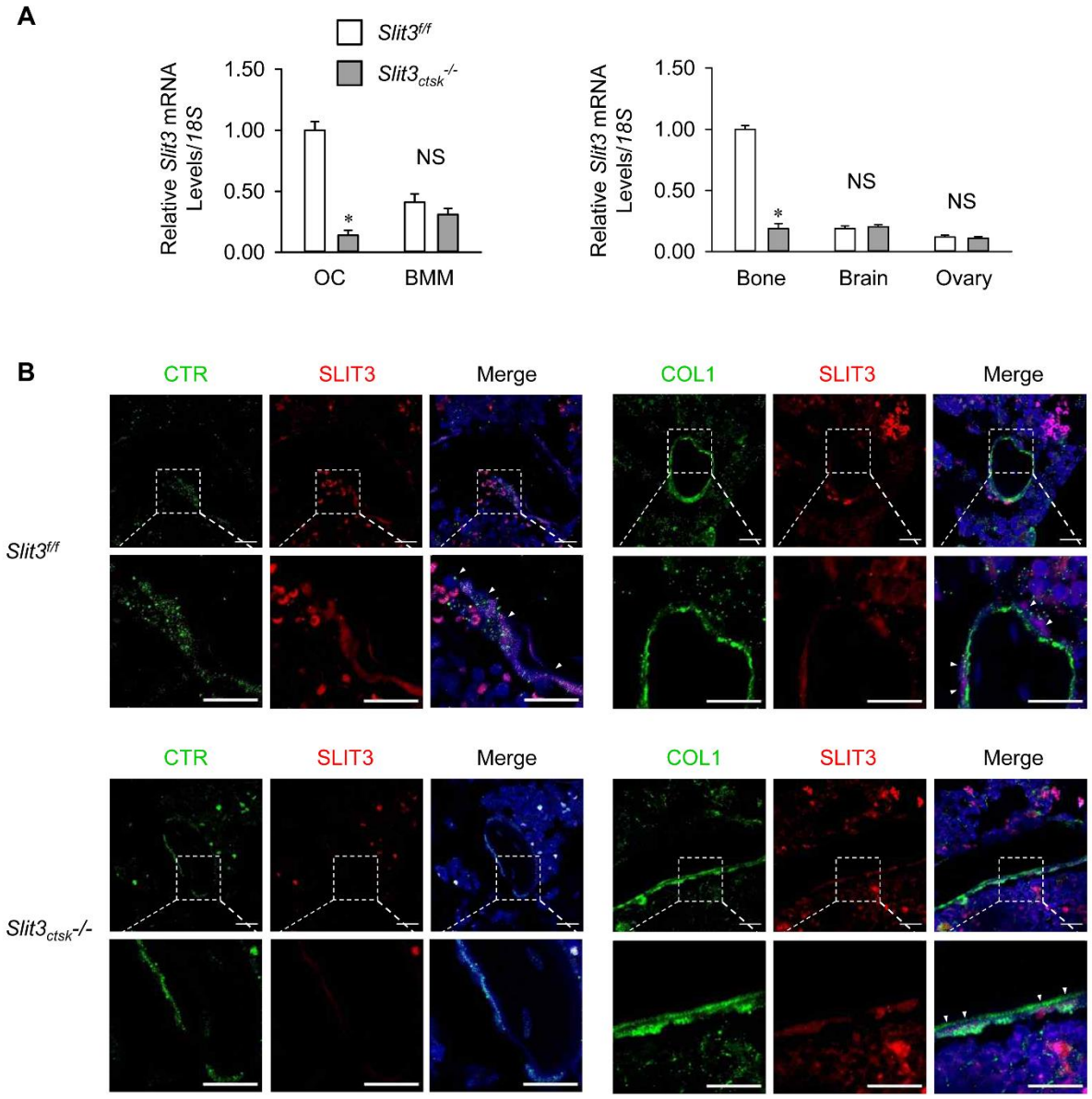
A
Slit3f/f
Slit3ctsk-/-
Relative Slit3 mRNA Levels/18S
1.50
1.00
0.50
0.00
NS
*
OC
BMM
Bone
Brain
Ovary
B
CTR
SLIT3
Merge
COL1
Slit3f/f
Slit3ctsk-/-
C
Ctsk-cre
WT
BV/TV (%)
Tb.Th (μm)
Tb.N (N/mm)
Tb.Sp (μm)
20.0
15.0
10.0
5.0
0.0
80
60
40
20
0
4.0
3.0
2.0
1.0
250
200
150
100
50

Supplemental Figure 8. Generation of Osteoclast-specific *Slit3*-deficient Mice

(A) Quantitative RT-PCR analysis of *Slit3* expression in osteoclasts (OC) and bone marrow macrophages (BMM) obtained from 6-week-old male $Slit3_{ctsk}^{-/-}$ and their $Slit3^{f/f}$ littermates (n = 3 per group). *Slit3* expression in the brains and ovaries of 16-week-old female mice was also assessed in comparison with the femurs. **(B)** IHC staining to determine SLIT3 expression in osteoblasts and osteoclasts. Immunofluorescence images of calcitonin receptor (CTR, left green) or collagen type 1 (COL1, right green) and SLIT3 (red) expression in the femurs of 12-week-old male $Slit3_{ctsk}^{-/-}$ and their $Slit3^{f/f}$ littermates (n = 3 per group) are shown. SLIT3 was found around both cell types at the bone surface (white, arrowheads) in $Slit3^{f/f}$ littermates but not in CTR-expressing osteoclasts in $Slit3_{ctsk}^{-/-}$ mice. Representative enlarged images from inset in top panels (bottom panels); ×2.5 magnifications. Scale bar, 50 μm. **(C)** Microcomputed tomography analyses of the femurs of 12-week-old female *cathepsin K-cre* (*Ctsk-cre*) mice and their wild-type littermates (n = 4 per group). Trabecular and cortical bone parameters were assessed. Bone volume/tissue volume (BV/TV), trabecular thickness (Tb.Th), trabecular number (Tb.N), and trabecular separation (Tb.Sp). Error bars denote the mean ± SEM. $^{*}p < 0.05$ *vs*. littermate control using the Mann–Whitney U-test. NS, not significant.

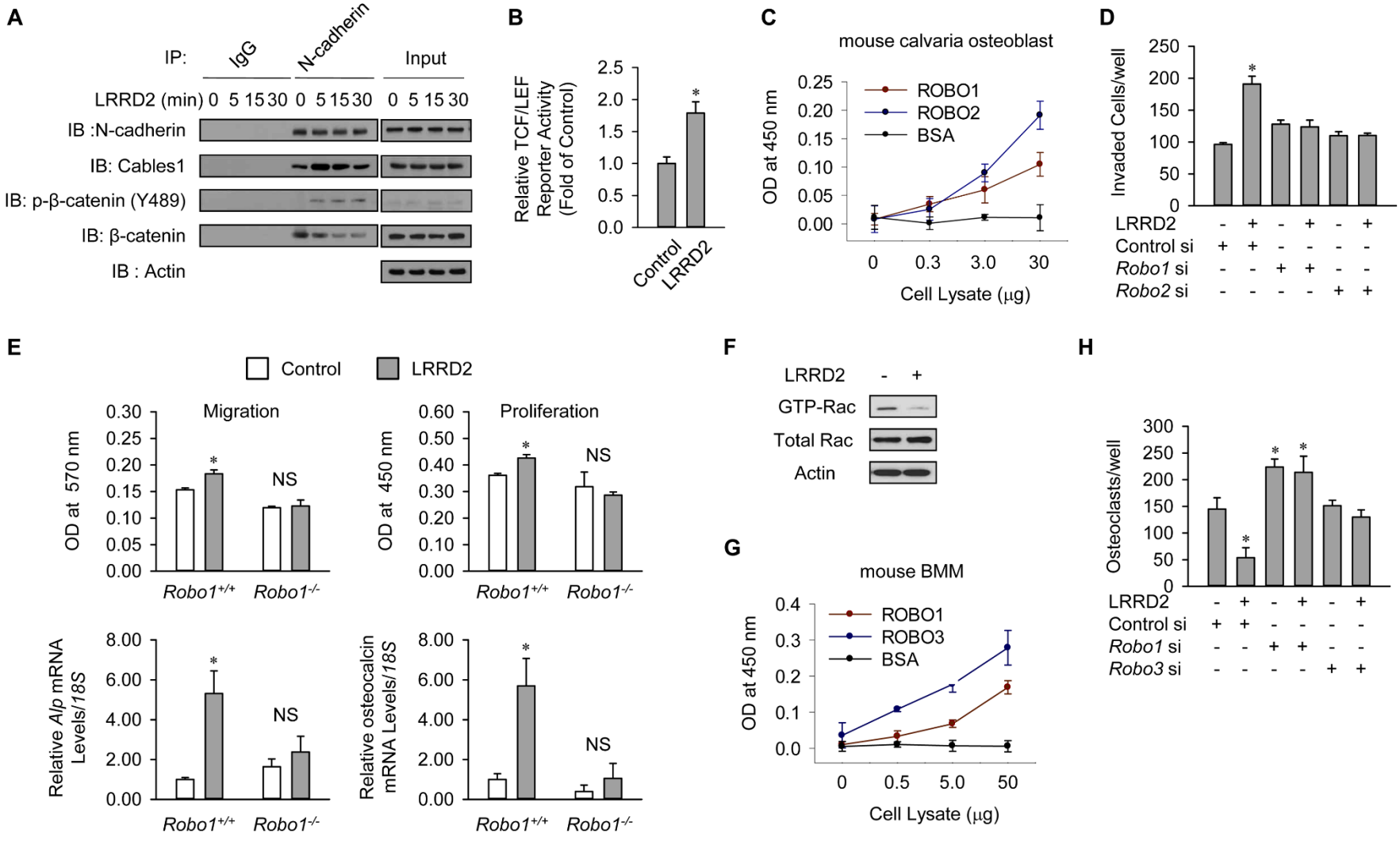
A
IP:
IgG
N-cadherin
Input
LRRD2 (min) 0 5 15 30 0 5 15 30 0 5 15 30
IB :N-cadherin
IB: Cables1
IB: p-β-catenin (Y489)
IB: β-catenin
IB : Actin
B
Relative TCF/LEF Reporter Activity (Fold of Control)
Control
LRRD2
C
mouse calvaria osteoblast
OD at 450 nm
ROBO1
ROBO2
BSA
Cell Lysate (μg)
D
Invaded Cells/well
LRRD2
Control si
Robo1 si
Robo2 si
E
Control
LRRD2
Migration
OD at 570 nm
Proliferation
OD at 450 nm
NS
Robo1+/+
Robo1-/-
Relative Alp mRNA Levels/18S
Relative osteocalcin mRNA Levels/18S
F
LRRD2
GTP-Rac
Total Rac
Actin
G
mouse BMM
OD at 450 nm
ROBO1
ROBO3
BSA
Cell Lysate (μg)
H
Osteoclasts/well
LRRD2
Control si
Robo1 si
Robo3 si

Supplemental Figure 9. Receptors and Signals for the Second Leucine-rich Repeat Domain (LRRD2) of Human SLIT3 in Osteoblasts and Osteoclasts

(A) Western blotting analysis of Cables, phosphorylated β-catenin at Y489, and total β-catenin after immunoprecipitation (IP) with N-cadherin in mouse calvaria osteoblasts with or without 10 nM LRRD2 treatment for the indicated variable times. **(B)** TCF/LEF reporter assay to monitor the β-catenin activity induced by 10 nM LRRD2 for 48 h in MC3T3-E1 cells. **(C and G)** Interaction of LRRD2 with ROBO1–3 in mouse calvaria osteoblasts (OB) (C) and mouse bone marrow macrophages (BMM) (G) using a binding ELISA assay. Various amounts of cell lysates were incubated for 2 h in LRRD2- or BSA-coated wells, followed by assay of the ROBO1–3 levels by ELISA. **(D)** The LRRD2 (10 nM)-stimulated directional migration of mouse calvaria OBs with or without *Robo1* siRNA or *Robo2* siRNA was assessed using a Boyden chamber system. The LRRD2 treatment was for 24 h, and the invaded cell numbers were counted. **(E)** Biological changes in the mouse calvaria OBs induced by 10 nM LRRD2. The OBs were obtained from 6-week-old *Robo1*$^{-/-}$ mice and their littermates (n = 3 in per group). Directional migration was assessed using a Boyden chamber system after treatment with LRRD2 for 24 h, and the extent of invasion was quantified by absorbance at 570 nm of crystal violet staining in invaded cells. Proliferation was measured using BrdU incorporation after treatment with LRRD2 for 48 h. Differentiation was assessed by quantitative RT-PCR analysis of *alkaline phosphatase* (*Alp*) and *osteocalcin* after treatment with LRRD2 for 7 days. **(F)** Western blotting analysis of Rac following treatment with 10 nM LRRD2 for 15 min in mouse BMMs exposed to 15 ng/ml M-CSF and 15 ng/ml RANKL. **(H)** LRRD2 (10 nM)-mediated suppression of osteoclastogenesis with or without *Robo1* siRNA or *Robo3* siRNA. Cells were treated with LRRD2 for 4 days in conjunction with 15 ng/ml M-CSF and 15 ng/ml RANKL, and TRAP-positive cells with more than three nuclei were

counted. Error bars denote the mean ± SEM. In vitro experiments were performed 3 times independently. $^{*}p < 0.05$ *vs*. untreated control using the Mann–Whitney U-test or Kruskal–Wallis test followed by Bonferroni correction. NS, not significant.

Supplemental Table 1. Identification of SLIT3 in Conditioned Media Collected from Differentiated Osteoclast-like Cells

1	MALGRTGAGA AVRARLALGL ALASILSGPP AAACPTKCTC SAASVDCHGL
51	GLRAVPRGIP RNAERLDLDR NNITRITKMD FAGLKNLRVL HLEDNQVSII
101	ERGAFQDLKQ LERLRLNKNK LQVLPELLFQ STPKLTRLDL SENQIQGIPR
151	KAFRGVTGVK NLQLDNNHIS CIEDGAFRAL RDLEILTLNN NNISRILVTS
201	FNHMPKIRTL RLHSNHLYCD CHLAWLSDWL RQRRTIGQFT LCMAPVHLRG
251	FSVADVQKKE YVCPGPHSEA PACNANSLSC PSACSCSNNI VDCRGKGLTE
301	IPANLPEGIV EIRLEQNSIK SIPAGAFTQY KKLKRIDISK NQISDIAPDA
351	FQGLKSLTSL VLYGNKITEI PKGLFDGLVS LQLLLLNANK INCLRVNTFQ
401	DLQNLNLLSL YDNKLQTISK GLFVPLQSIQ TLHLAQNPFV CDCHLKWLAD
451	YLQDNPIETS GARCSSPRRL ANKRISQIKS **KKFRCSGSED YR**NRFSSECF
501	MDLVCPEKCR CEGTIVDCSN QKLARIPSHL PEYTTDLRLN DNDISVLEAT
551	GIFKKLPNLR KINLSNNRIK EVREGAFDGA AGVQELMLTG NQLETMHGRM
601	FRGLSSLKTL MLRSNLISCV SNDTFAGLSS VRLLSLYDNR ITTITPGAFT
651	TLVSLSTINL LSNPFNCNCH MAWLGRWLRK RRIVSGNPRC QKPFFLKEIP
701	IQDVAIQDFT CDGNEESSCQ LSPRCPEQCT CVETVVRCSN RGLHALPKGM
751	PKDVTELYLE GNHLTAVPKE LSAFRQLTLI DLSNNSISML TNHTFSNMSH
801	LSTLILSYNR LRCIPVHAFN GLRSLRVLTL HGNDISSVPE GSFNDLTSLS
851	HLALGTNPLH CDCSLRWLSE WVKAGYKEPG IARCSSPESM ADRLLLTTPT
901	HRFQCKGPVD INIVAKCNAC LSSPCKNNGT CSQDPVEQYR CTCPYSYKGK
951	DCTVPINTCV QNPCEHGGTC HLSENLRDGF SCSCPLGFEG QRCEINPDDC
1001	EDNDCENSAT CVDGINNYAC LCPPNYTGEL CDEVIDYCVP EMNLCQHEAK
1051	CISLDKGFRC ECVPGYSGKL CETNNDDCVA HKCRHGAQCV DEVNGYTCIC
1101	PQGFSGLFCE HPPPMVLLQT SPCDQYECQN GAQCIVVQQE PTCRCPPGFA
1151	GPRCEKLITV NFVGKDSYVE LASAKVRPQA NISLQVATDK DNGILLYKGD
1201	NDPLALELYQ GHVRLVYDSL SSPPTTVYSV ETVNDGQFHS VELVMLNQTL
1251	NLVVDKGAPK SLGKLQKQPA VGSNSPLYLG GIPTSTGLSA LRQGADRPLG
1301	GFHGCIHEVR INNELQDFKA LPPQSLGVSP GCKSCTVCRH GLCRSVEKDS
1351	VVCECHPGWT GPLCDQEARD PCLGHSCRHG TCMATGDSYV CKCAEGYGGA
1401	LCDQKNDSAS ACSAFKCHHG QCHISDRGEP YCLCQPGFSG HHCEQENPCM
1451	GEIVREAIR**R QKDYASCATA SKV**PIMEC**RG GCGSQCCQPI RSKR**RKYVFQ
1501	CTDGSSFVEE VERHLECGCR ACS

Among the sequences of the SLIT3 protein, those of the peptides identified by LC-MS/MS are highlighted in bold red-colored text.

Supplemental Table 2. Baseline Characteristics of the 4,877 Postmenopausal Women Included in the Genetic Study

Variables	Discovery set			Replication set
	Control	Severe-low BMD	p	Subjects
	(n = 501)	(n = 481)		(n = 3,895)
Age (years)	58.4 ± 6.3	58.8 ± 7.0	0.346	60.2 ± 10.2
Height (cm)	154.9 ± 4.8	154.6 ± 5.2	0.255	154.1 ± 5.9
Weight (kg)	**54.5 ± 5.9**	**55.6 ± 6.7**	**0.006**	56.5 ± 8.3
BMI (kg/m^2)	**22.7 ± 2.6**	**23.3 ± 2.9**	**0.001**	23.8 ± 3.2
BMD (g/cm^2)				
Lumbar spine	**0.956 ± 0.005**	**0.727 ± 0.005**	**<0.001**	0.873 ± 0.003
Femur neck	**0.749 ± 0.004**	**0.635 ± 0.004**	**<0.001**	0.715 ± 0.002
T-score				
Lumbar spine	**–1.2 ± 0.9**	**–3.2 ± 0.7**	**<0.001**	–1.7 ± 1.4
Femur neck	**–1.1 ± 0.7**	**–2.3 ± 0.8**	**<0.001**	–1.3 ± 1.1
Osteoporosis, number (%)	**0**	**482 (100%)**	**<0.001**	1313 (33.7%)

BMI, body mass index; BMD, bone mineral density.

Supplemental Table 3. Common Functioning Variants (Minor Allele Frequencies ≥ 1%) Associated with Osteoporosis Prevalence in the Discovery Stage

Gene	Location	rs number	Genotype			MAF	HWE[A]	Dominant		Recessive		Co-dominant	
								OR (95% CI)	p[B]	OR (95% CI)	p	OR (95% CI)	p
SLIT2	Start gained	rs7655084	TT 859	GT 121	GG 2	0.064	0.429	**1.66 (1.13–2.44)**	**0.011**	∞	0.980	**1.67 (1.15–2.45)**	**0.008**
SLIT3	Exon	rs10036727	TT 357	CT 487	CC 138	0.388	0.179	1.08 (0.83–1.41)	0.547	**0.65 (0.45–0.94)**	**0.022**	0.93 (0.77–1.12)	0.450

[A]χ^2 tests were used to determine whether individual variants were in equilibrium at each locus in the population.

[B]Multiple logistic analyses using three alternative models after adjustments for age, weight, and height.

MAF, minor allele frequency; HWE, Hardy-Weinberg equilibrium; OR, odds ratio; 95% CI, 95% confidence interval.

Supplemental Table 4. Baseline Characteristics of the 346 Postmenopausal Women in Whom Circulating SLIT3 Levels were Measured

Variables	Mean ± SD
SLIT3 (ng/ml)	7.00 ± 2.34
Age (years)	59.6 ± 7.1
Weight (kg)	55.6 ± 6.9
Height (cm)	155.2 ± 5.7
Current smoker, no. (%)	5 (1.4)
Alcohol intake ≥ 3 U/day, no. (%)	2 (0.6)
Exercise ≥ 30 min/day, no. (%)	163 (47.1)
Bone mineral density (g/cm^2)	
Lumbar spine	0.882 ± 0.099
Femur neck	0.760 ± 0.085
Total femur	0.819 ± 0.091
Trochanter	0.641 ± 0.084
Shaft	0.993 ± 0.119
Ward's triangle	0.556 ± 0.092

Supplemental Table 5. Human Sequence of the Second Leucine-rich Repeat Domain (LRRD2) of SLIT3

1	MAPGWAGVGA AVRARLALAL ALASVLSGPP AVACPTKCTC SAASVDCHGL
51	GLRAVPRGIP RNAERLDLDR NNITRITKMD FAGLKNLRVL HLEDNQVSVI
101	ERGAFQDLKQ LERLRLNKNK LQVLPELLFQ STPKLTRLDL SENQIQGIPR
151	KAFRGITDVK NLQLDNNHIS CIEDGAFRAL RDLEILTLNN NNISRILVTS
201	FNHMPKIRTL RLHSNHLYCD CHLAWLSDWL RQRRTVGQFT LCMAPVHLRG
251	FNVADVQKKE YVCPAPHSEP PSCNANSISC PSPCTCSNNI VDCRGKGLME
301	IPANLPEG**IV EIRLEQNSIK AIPAGAFTQY KKLKRIDISK NQISDIAPDA**
351	**FQGLKSLTSL VLYGNKITEI AKGLFDGLVS LQLLLLNANK INCLRVNTFQ**
401	**DLQNLNLLSL YDNKLQTISK GLFAPLQSIQ TLHLAQNP**FV CDCHLKWLAD
451	YLQDNPIETS GARCSSPRRL ANKRISQIKS KKFRCSGSED YRSRFSSECF
501	MDLVCPEKCR CEGTIVDCSN QKLVRIPSHL PEYVTDLRLN DNEVSVLEAT
551	GIFKKLPNLR KINLSNNKIK EVREGAFDGA ASVQELMLTG NQLETVHGRV
601	FRGLSGLKTL MLRSNLISCV SNDTFAGLSS VRLLSLYDNR ITTITPGAFT
651	TLVSLSTINL LSNPFNCNCH LAWLGKWLRK RRIVSGNPRC QKPFFLKEIP
701	IQDVAIQDFT CDGNEESSCQ LSPRCPEQCT CMETVVRCSN KGLRALPRGM
751	PKDVTELYLE GNHLTAVPRE LSALRHLTLI DLSNNSISML TNYTFSNMSH
801	LSTLILSYNR LRCIPVHAFN GLRSLRVLTL HGNDISSVPE GSFNDLTSLS
851	HLALGTNPLH CDCSLRWLSE WVKAGYKEPG IARCSSPEPM ADRLLLTTPT
901	HRFQCKGPVD INIVAKCNAC LSSPCKNNGT CTQDPVELYR CACPYSYKGK
951	DCTVPINTCI QNPCQHGGTC HLSDSHKDGF SCSCPLGFEG QRCEINPDDC
1001	EDNDCENNAT CVDGINNYVC ICPPNYTGEL CDEVIDHCVP ELNLCQHEAK
1051	CIPLDKGFSC ECVPGYSGKL CETDNDDCVA HKCRHGAQCV DTINGYTCTC
1101	PQGFSGPFCE HPPPMVLLQT SPCDQYECQN GAQCIVVQQE PTCRCPPGFA
1151	GPRCEKLITV NFVGKDSYVE LASAKVRPQA NISLQVATDK DNGILLYKGD
1201	NDPLALELYQ GHVRLVYDSL SSPPTTVYSV ETVNDGQFHS VELVTLNQTL
1251	NLVVDKGTPK SLGKLQKQPA VGINSPLYLG GIPTSTGLSA LRQGTDRPLG
1301	GFHGCIHEVR INNELQDFKA LPPQSLGVSP GCKSCTVCKH GLCRSVEKDS
1351	VVCECRPGWT GPLCDQEARD PCLGHRCHHG KCVATGTSYM CKCAEGYGGD
1401	LCDNKNDSAN ACSAFKCHHG QCHISDQGEP YCLCQPGFSG EHCQQENPCL
1451	GQVVREVIRR QKGYASCATA SKVPIMECRG GCGPQCCQPT RSKRRKYVFQ
1501	CTDGSSFVEE VERHLECGCL ACS

Among the sequences of the SLIT3 protein, those of LRRD2 are highlighted in bold red-colored text.

Supplemental Table 6. Microcomputed Tomography Analyses in Mice Treated with the Second Leucine-rich Repeat Domain (LRRD2) of Human SLIT3

	Control	28 μg LRRD2 once a week	4 μg LRRD2 once a day	2 μg LRRD2 twice a day
BV/TV (%)	4.24 ± 0.33	4.53 ± 0.25	5.12 ± 0.31	5.53 ± 0.34[A]
Tb.Th (μm)	28.9 ± 1.0	29.8 ± 1.1	31.3 ± 1.1	33.6 ± 1.0[A]
Tb.N (N/mm)	1.26 ± 0.13	1.49 ± 0.16	1.63 ± 0.15	1.90 ± 0.17[A]
Tb.Sp (μm)	716.5 ± 72.1	725.8 ± 60.4	615.3 ± 64.3	587.9 ± 98.4

Values are expressed as the mean ± SE. [A]Statistically significantly different from the untreated control. The female C57BL/6J mice were ovariectomized at 8 weeks of age, and LRRD2 (mean 0.192 mg/kg/day) was injected via the tail vein starting 3 days after ovariectomy and continuing for 4 weeks (n = 7 per group). The body weights just before LRRD2 treatment were almost equivalent between all of the treated- and control groups.

BV/TV, bone volume/tissue volume; Tb.Th, trabecular thickness; Tb.N, trabecular number; Tb.Sp, trabecular separation.

Supplemental Methods

Cell Culture

Primary mouse bone marrow cells were obtained by flushing the femur and tibia of 6-week-old ICR mice (Orient, Seongnam, Korea) and cultured at 37°C in α-minimum essential medium (α-MEM; Wel Gene, Daegu, Korea) containing 10% fetal bovine serum (FBS; Gibco, Grand Island, NY), 100 U/ml penicillin, and 100 μg/ml streptomycin in a humidified atmosphere with 5% CO_2. After a 24 h culture, non-adherent cells were collected and cultured in 96-well plates at a density of 4.0×10^4 cells/well. Bone marrow macrophages (BMMs) were cultured with 30 ng/ml macrophage colony-stimulating factor (M-CSF; R&D Systems Inc., Minneapolis, MN) for more than 3 days. Cells at this stage were regarded as osteoclast precursors. BMMs were fully differentiated into osteoclasts by incubation in culture with 15 ng/ml M-CSF and 15 ng/ml soluble receptor activator of nuclear factor-κB (NF-κB) ligand (RANKL; R&D Systems Inc.) for more than 4 days, with the culture medium changed every 2–3 days. Alternatively, osteoclast-like cells were generated from murine macrophage RAW264.7 cells (ATCC, Manassas, VA) by incubation with the same dosage of RANKL for more than 4 days.

To generate human osteoclasts, peripheral blood was obtained from normal healthy volunteers. Blood was diluted with an equal volume of α-MEM, and peripheral blood mononuclear cells were then isolated by centrifugation over a Lymphoprep™ (Axis-Shield, Oslo, Norway) density gradient. Mononuclear cells were then resuspended in autoMacs buffer, and CD14-positive monocytes were selected using the autoMacs magnetic cell separator (Miltenyi Biotech, Auburn, CA). Cells were cultured with 25 ng/ml M-CSF for 3 days and then further cultured with 25 ng/ml M-CSF and 30 ng/ml RANKL for 4–6 days.

Mouse bone marrow mesenchymal stem cells were isolated by flushing the femurs and

tibia of 6-week-old mice. Bone marrow cells were subsequently collected and cultured in 6-well plates at a density of 1.0×10^7 cells/well in α-MEM containing 10% FBS, 100 U/ml penicillin, and 100 μg/ml streptomycin. After 24 h in culture, non-adherent cells were removed and adherent cells were cultured for an additional 2 weeks with fresh complete medium.

Primary mouse osteoblasts were isolated by sequential collagenase digestion of calvaria obtained from newborn or 6-week-old mice and maintained in α-MEM containing 10% FBS. Mature osteoblasts were generated from mouse calvaria osteoblasts in the presence of 50 μg/ml ascorbic acid and 10 mM β-glycerophosphate for 10–14 days.

Murine pre-osteoblast MC3T3-E1 cells (ATCC) were cultured at 37°C in α-MEM containing 10% FBS, 100 U/ml penicillin, and 100 μg/ml streptomycin in a humidified atmosphere with 5% CO_2. The medium was changed every 2-3 days. Upon reaching 80% confluence, cells were subcultured with trypsin-EDTA (Gibco).

Human bone marrow stromal cells were isolated from ribs that were discarded at the time of open thoracotomy in patients without metabolic bone disease and were cultured in α-MEM containing 10% FBS, 100 U/ml penicillin, and 100 μg/ml streptomycin.

Mouse Genotyping

For the PCR analysis of *Slit3*$^{-/-}$ mice, three primers were used. The wild-type allele amplified a 250-bp fragment (primers a and b), whereas the null allele amplified a 410-bp fragment (primers a and c). PCR conditions were 40 cycles at 94°C for 30 s, 68.5°C for 30 s, and 72°C for 1 min. The oligonucleotide sequences used for *Slit3*$^{-/-}$ mice were primer a (5′ GCG CCT CCT CGG GCT CCT CGT GTC 3′, sense), primer b (5′ TGC GGG GGA TGC CCC GAG GAA 3′, antisense), and primer c (5′ CGG ATT CTC CGT GGG AAC AAA CGG 3′, antisense). For the PCR analysis of

Robo1$^{-/-}$ mice, three primers were used. The wild-type allele amplified a 200-bp fragment (primers d and e), whereas the null allele amplified a 400-bp fragment (primers d and f). PCR conditions were 40 cycles at 94°C for 30 s, 63.5°C for 30 s, and 72°C for 1 min. The oligonucleotide sequences used for *Robo1*$^{-/-}$ mice were primer d (5′ TGG CAC GAA GGT ATA TGT GC 3′, sense), primer e (5′ GAA GGA CTG GTG GTT TTG AG 3′, antisense), and primer f (5′ CCT CCG CAA ACT CCT ATT TC 3′, antisense). For the PCR analysis of *Slit3*$^{f/f}$ mice, two primers were used. The wild-type allele amplified a 307-bp fragment, whereas the floxed allele amplified a 411-bp fragment (primers g and h). PCR conditions were 40 cycles at 94°C for 30 s, 56°C for 60 s, and 72°C for 1 min. The oligonucleotide sequences used for *Slit3*$^{f/f}$ mice were primer g (5′ TGT GAC TAG CAT GTA GTA GG 3′, sense) and primer h (5′ CCA GGC TCA GCC TTT TAG AG 3′, antisense). For the PCR analysis of *Cre* mice, two primers were used. The *Cre* transgene amplified a 100-bp fragment (primers i and j). PCR conditions were 35 cycles at 94°C for 30 s, 51.5°C for 60 s, and 72°C for 1 min. The oligonucleotide sequences used for *Cre* mice were primer i (5′ GCG GTC TGG CAG TAA AAA CTA TC 3′, sense) and primer j (5′ GTG AAA CAG CAT TGC TGT CAC TT 3′, antisense).

Chemotaxis

The chemotaxis assay was performed in a Boyden chamber system using a transwell with a polycarbonate membrane containing 8 μm pores (Costar, Corning, NY). Cells were seeded onto the inner chamber at a density of 1.0×10^5 cells per 100 μl in α-MEM with FBS for 6 h and then exposed to conditioned medium (CM), SLIT3 (R&D Systems Inc.), or LRRD2 in the outer chamber for an additional 24 h. The cells on the upper membrane were then completely removed by wiping with a cotton swab. The cells that invaded the lower membrane were fixed, stained with

hematoxylin, and counted using a computerized video-imaging system (Olympus, Tokyo, Japan). Alternatively, after staining of the invading cells with 1% crystal violet, 2% SDS was added for 30 min. The extracted crystal violet was then measured at an absorbance at 570 nm.

Measurement of Cell Proliferation

Cell proliferation was measured by 5-bromo-2′-deoxyuridine (BrdU) incorporation. Briefly, cells were cultured for various experimental times in the presence or absence of SLIT3 and/or siRNAs. Subsequently, the cells were incubated with BrdU for 6 h and proliferation was assayed using a BrdU labeling and detection kit (Roche, Mannheim, Germany).

Tartrate-resistant Acid Phosphatase Staining

Mouse BMMs were incubated with 15 ng/ml M-CSF and 15 ng/ml soluble RANKL for 4 days. Alternatively, 1.0×10^5 BMMs per well were co-cultured with 1.0×10^4 calvaria osteoblast cells per well on a type I collagen-coated 48 well plate in 0.4 ml/well of α-MEM containing 10% FBS, 10^{-8} M $1\alpha,25(OH)_2D_3$ (Sigma-Aldrich, St. Louis, MO) and 10^{-6} M PGE_2 (Sigma-Aldrich) for 14 days. Adherent cells were fixed and stained for tartrate-resistant acid phosphatase (TRAP), an enzymatic marker of osteoclasts, using a leukocyte acid phosphatase kit (Sigma-Aldrich) in accordance with the manufacturer's instructions. TRAP-positive multinucleated cells containing three or more nuclei were considered to be osteoclasts and were counted under a light microscope (Olympus). For the fusion assay, mouse BMMs were cultured with the same concentrations of M-CSF and RANKL for 2–3 days prior to actin ring formation. Osteoclast-like cells derived from RAW264.7 cells and human osteoclasts derived from peripheral blood mononuclear cells were also stained for TRAP.

Osteoclast Migration and Actin Ring Formation

Osteoclasts (0.5×10^3 cells/well in 96-well culture plates) were seeded onto dentin discs (IDS Ltd., Boldon, UK) in culture medium containing SLIT3 (1 μg/ml) in the presence of M-CSF (30 ng/ml) and RANKL (30 ng/ml) for 2 days. Following ultrasonication, the dentin slices were stained with hematoxylin (Sigma-Aldrich) for 1 min. The length of the resorbed pits was analyzed using Image-Pro Plus software (MediaCybernetics, Sliver Spring, MD).

For detection of the actin ring, osteoclasts were fixed with 4% paraformaldehyde for 20 min, permeabilized with 0.5% Triton X-100 in PBS for 5 min, and stained with FITC-conjugated phalloidin for 12 h at 4°C. After washing three times with PBS, the stained cells were mounted and photographed using a confocal laser scanning microscope (Zeiss LSM 710 confocal microscope, Germany).

Transfection with siRNA and Overexpression Vector

Slit3 siRNA (SI01425795; Qiagen, Hilden, Germany) and scrambled siRNA (AAG CAA CTA TCA CAT ACT CAC CT), β-catenin siRNA (MSS273500; Invitrogen) and scrambled siRNA (AAG AGC TGA CAA AGT CTC GCG AAG ATA), *Robo1* siRNA (MSS208673; Invitrogen), *Robo2* siRNA (MSS241005; Invitrogen), *Robo3* siRNA (SI01404431; Qiagen) and nonsense siRNA (Stealth RNAi™ siRNA negative control; Invitrogen), and *Rac1-V12* overexpression vector and empty vector (pCMV5; Cell Biolabs, San Diego, CA) were transfected into cells using Lipofectamine reagent (Invitrogen) according to the manufacturer's instructions. Briefly, after the incubation of cells in α-MEM containing 10% FBS, siRNA reagent mixtures in OPTI-MEM (Invitrogen) were added and the cells were further incubated for an additional 6 h. The medium

was then replaced with fresh complete α-MEM and the cells were further cultured for 24 h.

Determination of Mouse Serum and Cellular SLIT3 Concentrations

Cells were washed three times with serum- and phenol red-free medium, and the supernatant was replaced with 6 ml serum- and phenol red-free α-MEM for 1 day. The CM was filtered through a 0.45-μm membrane filter and stored at –70°C. Proteins in the CM were precipitated by lyophilization and their concentrations were then measured using the BCA protein assay kit (Pierce Chemical Co., Rockford, IL). The SLIT3 concentration was measured using a commercially available kit (SED353Mi; USCNK, Wuham, China) employing a quantitative sandwich enzyme immunoassay technique in accordance with the manufacturer's instructions. The intra-assay CV was < 10% and the inter-assay CV was < 12%. The detection range generated from the standard curve by the manufacturer was 0.156 to 10 ng/ml, and the minimum detectable dose of SLIT3 was typically less than 0.065 ng/ml. The mean values of duplicate samples were reported.

To determine the mouse serum SLIT3 concentration, mouse blood was allowed to clot for 20 min at room temperature. The clotted material was removed by centrifugation at 3,000 rpm for 10 min. To determine the bone marrow SLIT3 concentration, mouse bone marrow fluid was obtained from tibia by centrifugation at 6,000 rpm for 1 min, and then suspended in 100 μl ice-cold PBS. The cell-free supernatant was collected following centrifugation at 6,000 rpm for 1 min. The serum and bone marrow fluid were stored at –80°C until further analysis. The SLIT3 concentration was measured by enzyme-linked immunosorbent assay (ELISA). Plates (96-well) were coated with samples and standards in PBS and incubated overnight at 4°C. The plates were then washed three times with 300 μl PBST (0.05% Tween-20 in PBS) and incubated for 2 h at room temperature with 200 μl of blocking solution (1% bovine serum albumin [BSA] in PBST)

per well. After washing with PBST, 100 µl (2 µg/ml diluted in 0.1× blocking solution) of SLIT3 antibody (AF3629; R&D Systems Inc.) was added to each well and the plates were incubated for 2 h at room temperature. After further washing, 100 µl of polyclonal HRP-linked anti-goat antibody (diluted 1:10,000 in 0.1% BSA in PBST) was added to each well and the plates were incubated at room temperature for 1 h. The reaction was developed using successive incubations with 100 µl of TMB substrate solution followed by 50 µl of 2N H_2SO_4 to stop the reaction. Mouse recombinant SLIT3 was used to generate a standard curve. The detection range was 1.0 to 100 ng/ml. The lower detection limit was 0.5 ng/ml. The mean values of duplicate samples were reported.

Bone immunohistochemistry

For the immunohistochemical analysis of bone samples, freshly dissected bone tissues were immediately fixed in ice-cold 4% paraformaldehyde solution for 4 h. Decalcification was carried out with 0.5 M EDTA at 4℃ with constant shaking, and the decalcified bones were immersed into 20% sucrose and 2% polyvinylpyrrolidone solution for 24 h. Finally, the tissues were embedded and frozen in OCT compound. For immunofluorescent staining and morphological analyses, sections were generated using low-profile blades on a LeicaCM1860 cryostat. For phenotypic analysis, mutant and littermate control samples were always processed, sectioned, stained, imaged and analyzed together under the same conditions and settings. For immunostaining, bone sections were air-dried, permeabilized for 10 min in 0.3% Triton X-100, blocked in 5% donkey serum at room temperature for 30 min, and probed with the primary antibodies diluted in 5% donkey serum in PBS for 2 h at room temperature or overnight at 4℃. The following primary antibodies were

used: endomucin (sc-65495, Santa Cruz, diluted 1:100), CD31/pecam1 conjugated to Alexa Fluor 488 (FAB3628G, R&D Systems, 1:100), collagen type 1 (AB675P; Millipore, 1:200), calcitonin receptor (ab11042, Abcam, 1:200), and SLIT3 (782619, Novous Biologicals, 1:100). After primary antibody incubation, sections were washed three times with PBS and incubated with appropriate Alexa Fluor-coupled secondary antibodies (1:400, Molecular Probes) for 1 h at room temperature. Nuclei were counterstained with DAPI. Sections were thoroughly washed with water and mounted using FluoroMount-G (Southern Biotech).

Western Blotting and Immunoprecipitation Analyses

Total cell lysates were prepared in lysis buffer (10 mM sodium phosphate [pH 7.2], 150 mM NaCl, 1 mM EDTA, 1% NP-40, 1% Na-deoxycholate, 0.1% SDS, 1 mM PMSF, 1 mM Na_3VO_4, 1 mM NaF, and a protease inhibitor mixture) at 4°C for 20 min. For cell fractionation, cells were lysed in cytosolic protein extraction buffer (0.33M sucrose, 1mM MgCl2, 0.1% TritonX-100, 10mM HEPES [pH7.4]) and nuclear extraction buffer (0.45M NaCl, 10mM HEPES [pH7.4]). Protein concentrations was measured using the BCA protein assay kit (Pierce Chemical Co., Rockford, IL). Samples containing 10–20 μg protein were separated by SDS-polyacrylamide gel electrophoresis (SDS-PAGE) on 12% gels and then transferred to nitrocellulose membranes (Amersham Biosciences, Buckinghamshire, UK). After blocking with 5% skim milk in TBST (500 mM Tris-HCL [pH 7.4], 1.5 M NaCl, and 0.1% Tween-20) for 1 h at room temperature, the membranes were incubated overnight with primary antibodies at 4°C, and subsequently with secondary antibodies. Immunoreactive proteins were detected using an enhanced chemiluminescence kit (PerkinElmer, Waltham, MA). Antibodies against ROBO1 (ab7279) and ROBO3 (ab101811) were purchased from Abcam (Cambridge, MA). Antibodies against RhoA

(#2117), Cdc42 (#2462), and Rac1/2/3 (#2465) were purchased from Cell Signaling Technology (Beverly, MA). Antibodies against ROBO2 (RP2861) and β-catenin (CM1181) were purchased from ECM (Versailles, KY). Antibodies against SLIT3 (PAB11260), active β-catenin (#05-665), and β-actin (A2228) were purchased from Abnova, Millipore (Billerica, MA) and Sigma-Aldrich, respectively.

For immunoprecipitation, cells were lysed with TNE buffer (25 mM Tris-HCl [pH 7.4], 150 mM NaCl, 1% Triton X-100, and 1 mM EDTA) containing a protease inhibitor cocktail (Sigma-Aldrich) and phosphatase inhibitors (1 mM Na_3VO_4 and 1 mM NaF). Cell lysates (1 mg protein per IP) were pre-cleared by incubation with 20 µl Protein-A or G-Sepharose beads (Amersham Biosciences) and control IgG (1 µg, Sigma) per ml for 1 h to remove nonspecific binding. The cleared lysates were incubated with primary antibody and Protein-A or G-Sepharose beads for 4 hr to overnight, at 4°C. The immunoprecipitates and cell lysates were collected by centrifugation, washed in 4× TNE buffer and denaturated with 2× SDS sample buffer. Denaturated proteins were separated by SDS-PAGE and detected by immunoblotting. In some experiments, the primary antibody step was followed by incubation with a horseradish peroxidase-conjugated antibody that recognizes rabbit or mouse IgG (#18-8816-31, 18-8817-31 TrueBlot™, eBioscience, San Diego, CA) to reduce immunglobulin heavy and light chains. Antibodies against N-cadherin, Cables1, phospho-β-catenin (Y489) and β-catenin were purchased from Abcam (ab76057) or Cell signaling (#14215), Santa Cruz Biotechnology (M-280), Abcam (ab119801) and ECM Biosciences (CM1181), respectively.

Semiquantitative and Quantitative Reverse-transcription PCR

Total RNA was purified using TRIzol reagent (Invitrogen) in accordance with the manufacturer's

instructions, and cDNA was synthesized from 1 μg of total RNA using the Superscript III First-Strand Synthesis System (Invitrogen). All PCR amplifications were performed using a Biometra thermal cycler (Göttingen, Germany). The level of mRNA expression of each target gene was normalized to that of a housekeeping gene using the Quantity One program. The specific primer pairs used were as follows: 5′ AGG GAA GCC TAC GCA GAT G 3′ (sense) and 5′ TGG ACA GTG GGC GAT TTT AT 3′ (antisense) for *Robo1*; 5′ AGC CCC ACA CAA ACA AGG 3′ (sense) and 5′ AAG CTG GGC TTG CTG TAG G 3′ (antisense) for *Robo2*; 5′ GCA GCG CTC AAC CCT AGT 3′ (sense) and 5′ CTT CTG GCC CAA CTC TTG AC 3′ (antisense) for *Robo3*; 5′ CGC ATG TCT CTG ACC CCT AC 3′ (sense) and 5′ GAG CTG TTA GCT TGG TGC AA 3′ (antisense) for *Robo4*; 5′ CGA CCA TTG TTA GCC ACA TAC G 3′ (sense) and 5′ TCG TCC TGA AGA TAC TGC AGG TT 3′ (antisense) for *Trap*; 5′ AGT TGC CCT CTT ATG AAG GAG AAG 3′ (sense) and 5′ GGA GTG TCG TCC CAG CAC AT 3′ (antisense) for *Ctr*; 5′ TTG CCG CTG TGG ACT ATC TG 3′ (sense) and 5′ GAA TGC AGC TCG GTT CAA AC 3′ (antisense) for *Dc-stamp*; and 5′ ACT TTG TCA AGC TCA TTT CC 3′ (sense) and 5′ TGC AGC GAA CTT TAT TGA TG 3′ (antisense) for *Gapdh*. The amplification protocol consisted of 30 cycles of denaturation at 95°C for 30 s, annealing at 60°C for 30 s, and extension at 72°C for 30 s. PCR products were separated on 1.5% agarose gels, stained with ethidium bromide, and visualized under UV light.

Quantitative PCR was performed using the Light Cycler 480 (Roche). The gene expression levels were determined using a Light Cycler 480 SYBR Green I Master Mix (Roche) and Probes Master Mix (Roche). PCR amplification was performed in duplicate samples, and a negative control was generated in each run by replacing the cDNA with water. The specific primer sequences and probes used were as follows: 5′ TGG CTG TGC CCA GTG CGT AT 3′ (sense) and 5′ CGC TGG GAA GGC AGC TCA GT 3′ (antisense) for *Slit1*; 5′ ACT TAA GTT GCC CAC

GGA TCT TCT G 3′ (sense) and 5′ ATG GGG CAG GAG AGC TGA CAG 3′ (antisense) for *Slit2*; 5′ GCT TGT GCA CCA TGG CCC 3′ (sense) and 5′ CTC TCC AGC TGC TTC AGA TC 3′ (antisense) for *Slit3*; 5′ CGA CCA TTG TTA GCC ACA TAC G 3′ (sense) and 5′ TCG TCC TGA AGA TAC TGC AGG TT 3′ (antisense) for *Trap*; 5′ ATA TGT GGG CCA GGA TGA AAG TT 3′ (sense) and 5′ TCG TTC CCC ACA GGA ATC TCT 3′ (antisense) for *CatK*; 5′ TGT CTG GAG ATT CGA CTT GAA GTC 3′ (sense) and 5′ TGA GTT CCA GGG CAC ACC A 3′ (antisense) for *Mmp9*; 5′ AGT TGC CCT CTT ATG AAG GAG AAG 3′ (sense) and 5′ GGA GTG TCG TCC CAG CAC AT 3′ (antisense) for *Ctr*; 5′ CTC AAC ACG GGA AAC CTC AC 3′ (sense) and 5′ CGC TCC ACC AAC TAA GAA CG 3′ (antisense) for *18S*; 5’ GGA GTT CAA GGC CCT GCA GG 3’ (sense) and 5’ CCT TCT CAC TCA GCA CCC GC 3’ (antisense) for *RpII*; *Alp* (Mm00475834_m1; ABI); osteocalcin (Mm03413826_mH; ABI); β-catenin (Mm00483039_m1; ABI); and *18S* (Hs03928990_g1; ABI). The reaction protocol was as follows: preincubation at 95°C for 10 min to activate FastStart DNA polymerase, followed by 45 reaction cycles comprising 10 s at 95°C, 15 s at 55°C, and 20 s at 72°C. Results were normalized to *18S*.

Bone Marrow Cavity Transplantation

Eleven-week-old C57BL/6 mice (Orient) were used for bone marrow cavity transplantation. Mice were anesthetized and irradiated (5.0 Gy) on the lower limbs. After 3 days, the tibias were gently drilled with a 26-gauge needle. MC3T3-E1 cells or BMMs were infected with adenovirus-GFP or -RFP for 24 h and the GFP- or RFP-labeled cells were then injected into the bone marrow cavity alongside PBS (left tibia) or 300 μg/kg SLIT3 (right tibia) using a 31-gauge needle. The mice were sacrificed after 3 days, and the tibias were fixed in 4% paraformaldehyde. Each tibia was decalcified in 14% EDTA and embedded in OCT compound for the generation of frozen sections.

Samples were observed using a fluorescence microscope (Olympus) to count the number of GFP- or RFP-positive cells out of the assumed injection sites. Ten sections per mouse were reviewed.

SLIT3/LRRD2-ROBO Binding Assay

Recombinant SLIT proteins (10 µg/ml) or SLIT3 second leucine-rich repeat (LRRD2) (2.5 µg/ml) were coated onto 96-well microtiter plates for 18 h at 4°C. Each well was washed three times with 300 µl PBST washing solution (0.05% Tween-20 in PBS), and plates were subsequently blocked with 1% BSA in PBST for 2 h at room temperature. After washing with PBST, cell lysate was added for 2 h and the wells were then washed three times. ROBO antibody (1:1000) was added for 2 h in blocking solution. After washing, HRP-linked antibody (Cell signaling, 1:2000) was added for 2 h and plates were then washed five times. The reaction was developed by successive incubations with 100 µl of TMB substrate solution and 100 µl of 1 N H_2SO_4 to stop the reaction.

Construction of Luciferase Reporter Genes and the Luciferase Assay

The –2341/+60 *Slit3* promoter region was amplified from mouse genomic DNA by PCR and used to construct the promoter-luciferase reporter. The primers for promoter amplification were as follows: forward (–2341) primer 5′ GGA AGA TCT AGG TAC CGA GCG CCC 3′, and reverse (+60) primer 5′ CGA CGC GTG TGA GCA CCA GAA GGA G 3′. Plasmid construct integrity was confirmed by DNA sequencing. For the luciferase reporter assay, RAW264.7 cells were cultured in α-MEM supplemented with 10% FBS. Transfections were performed in 24-well plates using Lipofectamine reagent in accordance with the manufacturer's protocol. Each transfection experiment also included 50 ng pActin-βgal plasmid to control for the transfection efficiency.

Activation of Wnt/β-catenin was confirmed using a SuperTOPFlash luciferase reporter

assay. MC3T3-E1 cells were transfected with 100 ng 8× SuperTOPFlash (provided by Aimee D. Kohn, M.D., Ph.D., SCCA Evergreen Health, Kirkland, WA) in 24-well plates using Lipofectamine reagent. After 48 h, cell lysates were assayed with the Dual Luciferase kit (Promega, Madison, WI). Relative activity was calculated as the ratio of the firefly reporter to the Renilla luciferase control. Luciferase activity was measured using a luminometer (Centro LB 960; Berthold Technologies, Bad Wildbad, Germany).

Chromatin Immunoprecipitation

Chromatin immunoprecipitation (ChIP) assays were performed as described previously, with minor modifications (1). Briefly, RAW264.7 cells were exposed to 100 ng/ml RANKL for 1 h and then fixed with 1% formaldehyde for 15 min at room temperature. Cells were washed with cold PBS and resuspended in lysis buffer (50 mM Tris-HCl [pH 8.0], 1% SDS, and 10 mM EDTA). Soluble chromatin was prepared by sonication and immunoprecipitated using antibodies against NF-κB p50 (sc-8414x; Santa Cruz Biotechnology), phosphorylated cAMP response element-binding protein (CREB; Cell Signaling), or preimmune IgG. The final DNA extractions were analyzed by PCR using the following primers: forward (–1039) 5′ CCT GTA ACA TGG CCC TTC CC 3′ and reverse (–744) 5′ GAA CTT GGA CCC CGG TAT TGA C 3′; forward (–330) 5′ CGG GCT GGC CAA GTC CCT T 3′ and reverse (–52) 5′ CTG GGC TGC GGA GCA CAG 3′; and forward (exon) 5′ GAA TCC ATG TAT GGG GGA GAT AG 3 ′ and reverse (exon) 5′ ACG CGC GGC AGC CAC ATT 3 ′, encompassing a control region with no binding sites for p50 and CREB.

GTPase Activity Assay

Activation of Rac, Cdc42, and RhoA was determined by precipitating activated Rac, Cdc42, and

RhoA-GTP from lysed cells using GST-fusion proteins (Rac/Cdc42: GST-Pak1.RBD, Millipore 41-325; RhoA: GST-RBP, Millipore 14-383). Cells were washed in PBS and lysed with 20 mM HEPES (pH 7.5), 150 mM NaCl, 5 mM EDTA, 1% NP-40, and a protease inhibitor cocktail. Cell lysates were clarified by centrifugation at 8,000 rpm for 5 min, and the supernatant was incubated with GST-fusion proteins on glutathione-agarose beads in a total volume of 0.5 ml for 60 min at 4°C with gentle agitation. Beads were then washed three times with lysis buffer and the bound proteins were eluted with sample protein buffer (2× concentration). Active protein expression levels were confirmed by western blot analysis using specific antibodies against Rac, Cdc42, and RhoA (Cell Signaling).

Measurement of Bone-specific Alkaline Phosphatase and C-terminal Telopeptide of Type I Collagen in Mice

Serum bone-specific alkaline phosphatase (ALP) concentration was used as a bone formation marker and was assessed using a commercially available ELISA kit (MBS028361, MyBioSource, San Diego, CA) with a lower detection limit of 0.24 ng/ml. Serum C-terminal telopeptide of type I collagen (C-telopeptide) concentration was used as a bone resorption marker and was also assessed using a commercially available ELISA kit (AC-06F1, RatLaps™ EIA; Immunodiagnostic Systems, Scottsdale, AZ) with a lower detection limit of 2.0 ng/ml. Kits were used in accordance with the manufacturers' instructions. The mean values of duplicates were reported.

Genetic Studies in Postmenopausal Women

Study Populations

The human study populations comprised three cohorts from the Asan, Catholic, and Kangwon Medical Centers (ACK-MC) in Korea. The AMC cohort comprised 2,922 postmenopausal Korean women who visited the AMC (2). The Catholic Medical Center (CMC) cohort consisted of 1,206 postmenopausal women from the Chungju suburb community (3). The Kangwon Medical Center (KMC) cohort consisted of 749 postmenopausal Korean women who visited the KMC (4).

Menopause was defined as the absence of menstruation for at least 1 year and was confirmed by measurement of serum follicle-stimulating hormone levels. Women who exhibited premature menopause (< 40 years of age) and those who had taken drugs that could affect bone metabolism for more than 6 months or within the previous 12 months before baseline visits, such as bisphosphonates, systemic glucocorticoid, or hormone-replacement therapy, were excluded from the study. Subjects with diseases that might affect bone metabolism, such as diabetes, cancer, hyperparathyroidism, and rheumatoid arthritis, were also excluded. Osteophyte formation above grade four on the Nathan classification and/or severe facet joint osteoarthritis in the lumbar spine, as determined by conventional spine radiographs, also led to subject exclusion. Subjects were excluded also if they had a fever (oral temperature ≥ 38.0°C) or abnormal findings on complete blood counts of leukocytes (< 4.0 or > 10.0×10^9/l) or platelets (< 150 or > 350×10^9/l). Finally, abnormal liver, kidney, or thyroid function, or abnormal serum concentrations of calcium, phosphorus, or ALP, were additional reasons for exclusion. These criteria were used to rule out individuals with systemic illness.

In the discovery stage of the study, targeted resequencing was performed on subjects from the AMC cohort who exhibited extreme phenotypes. Subjects were divided into two age-matched groups according to femoral neck (FN) bone mineral density (BMD) values and body mass index (BMI). Because a higher BMI is associated with a higher BMD, BMI criteria were intentionally

included to enhance the identification of genetic influence. The control group (n = 505) contained subjects with FN BMD values in the top 10% of age-matched subjects despite a relatively low BMI. The severe-low BMD group (n = 505) included those with FN BMD values in the bottom 10% of age-matched subjects despite a relatively high BMI. After quality control, 501 subjects in the control group and 481 subjects in the severe-low BMD group were selected for targeted resequencing. Replication genotyping was performed on the remaining subjects of the ACK-MC cohort (n = 3,895).

Targeted Resequencing

We focused on the *SLIT1* gene (NM_003061) on chromosome 10, *SLIT2* gene (NM_004787) on chromosome 4, *SLIT3* gene (NM_003062) on chromosome 5, *ROBO1* gene (NM_001145845) on chromosome 3, *ROBO2* gene (NM_NM_002942) on chromosome 3, *ROBO3* gene (NM_022370) on chromosome 11, and *ROBO4* gene (NM_019055) on chromosome 11. The target regions for these genes were the whole coding exons, exon-intron boundaries, and regulatory regions. Bait libraries were designed and assessed for coverage across these target genomic regions using the Agilent eArray website (https://earray.chem.agilent.com/earray/). The online design procedure recommended repeat masking of the target sequence to minimize off-target capture. The resulting baits were searched against the human genome reference (hg19). If a bait mapped to more than one location with a greater than 90% sequence identity using BLAST (~12 mismatches across the bait), it was removed from the design. Finally, 6,507-bp target regions were captured by the Agilent SureSelect Sequence Enrichment Kit. Subsequent sequencing with an Illumina HiSeq2000 analyzer (Illumina, San Diego, CA) was performed. Genomic DNA (3 μg) was randomly sheared using the Covaris System to generate inserts of about 150 bp. The fragmented DNA was end-

repaired using T4 DNA polymerase and Klenow polymerase, and Illumina paired-end adaptor oligonucleotides were ligated to the sticky ends. The ligation mixture was analyzed by agarose gel electrophoresis and fragments of 200–250 bp were isolated. To capture the targeted regions, the resulting purified DNA library was hybridized with a SureSelect Target Enrichment probes set (Agilent, Santa Clara, CA), in accordance with the manufacturer's instructions. The captured library was used to prepare a HiSeq2000 paired-end flow cell as described in the manufacturer's protocol. Clusters of PCR colonies were then sequenced using the HiSeq2000 platform.

Selection of Genetic Variants with Putative Functional Effects

To identify genetic variants that putatively affected gene function, non-synonymous single nucleotide polymorphisms (nsSNPs) or variants predicted to be "benign", "possibly damaging", or "probably damaging" by sequence- and structure-based predictions made using the Polymorphism Phenotyping (PolyPhen-2) version 2 software (v2.2.2) (5) and variants with the known transcription factor binding site by the University of California Santa Cruz (UCSC) Genome Browser database (http://genome.ucsc.edu/) (6) were selected for analysis of the replication stage.

Replication Genotyping

Genotyping was performed using the SNPtype^{TM} assay (Fluidigm, San Francisco, CA) according to the manufacturer's recommendations. Briefly, 75 ng genomic DNA was used for PCR amplification of a region containing the SNP of interest using an STA primer set and Qiagen 2× Multiplex PCR Master Mix (Qiagen) in a 5-µl reaction volume. PCR conditions were as follows: 1 cycle at 95°C for 15 min, then 14 cycles at 95°C for 15 s and 60°C for 4 min. After amplification,

products were diluted 1:100 in DNA Suspension Buffer. Diluted STA products (2.5 μl) were added to a Sample Pre-Mix containing 3 μl 2× Fast Probe Master Mix, 0.3 μl SNPtype™ 20× Sample Loading Reagent, 0.1 μl SNPtype™ Reagent, and 0.036 μl 50× ROX™ reference dye (Invitrogen). After the Assay Pre-Mix and the Sample Pre-Mix were loaded into the 96.96 Dynamic Array, the SNPtype™ assay reaction was carried out as follows: 1 cycle at 95°C for 5 min, 95°C for 15 s, 64°C for 45 s, 72°C for 15 s, 95°C for 15 s, 63°C for 45 s, 72°C for 15 s, 95°C for 15 s, 62°C for 45 s, 72°C for 15 s, 95°C for 15 s, 61°C for 45 s, and 72°C for 15 s, followed by 34 cycles at 95°C for 15 s, 60°C for 45 s, and 72°C for 15 s, and one final cycle at 25°C for 10 s. Analysis was carried out using Fluidigm SNP Genotyping Analysis software (version 3.1.1; Fluidigm).

Biomarker Study in Postmenopausal Women

Study Participants

Study subjects were selected from postmenopausal Korean women who visited AMC between January 2005 and June 2009. All women either visited an osteoporosis clinic for concerns regarding a possible diagnosis of osteoporosis or were referred for osteoporosis that had been detected during a routine examination. The same exclusion criteria of the genetic study were applied. After subject exclusion, 346 postmenopausal women were eligible for participation.

Measurement of Human Plasma SLIT3 Concentration

Fasting morning venous blood samples were obtained. After centrifugation, supernatants without cell components were collected, and all samples showing hemolysis or clotting were discarded. Plasma samples were stored at –80°C prior to assay. SLIT3 levels were assayed using a commercially available kit (SED353Mi; USCNK, Wuham, China) employing a quantitative

sandwich enzyme immunoassay technique in accordance with the manufacturer's instructions. The intra-assay CV was < 10% and the inter-assay CV was < 12%. The detection range generated from the standard curve by the manufacturer was 0.156 to 10 ng/ml, and the minimum detectable dose of SLIT3 was typically less than 0.065 ng/ml. The mean values of duplicate samples were reported.

Measurements of BMD

Measurements were performed as described previously (7).

Supplemental References

1. Orlando V, Strutt H, Paro R. Analysis of chromatin structure by in vivo formaldehyde cross-linking. *Methods.* 1997;11(2):205-214.
2. Estrada K, et al. Genome-wide meta-analysis identifies 56 bone mineral density loci and reveals 14 loci associated with risk of fracture. *Nat Genet.* 2012;44(5):491-501.
3. Kim G, et al. Relationship between vitamin D, parathyroid hormone, and bone mineral density in elderly Koreans. *J Korean Med Sci.* 2012;27(6):636-643.
4. Kim SW, Lee HA, Cho EH. Low handgrip strength is associated with low bone mineral density and fragility fractures in postmenopausal healthy Korean women. *J Korean Med Sci.* 2012;27(7):744-747.
5. Adzhubei IA, et al. A method and server for predicting damaging missense mutations. *Nat Methods.* 2010;7(4):248-249.
6. Meyer LR, et al. The UCSC Genome Browser database: extensions and updates 2013. *Nucleic Acids Res.* 2013;41(Database issue):D64-69.
7. Kim BJ, et al. Plasma sphingosine 1-phosphate levels and the risk of vertebral fracture in postmenopausal women. *J Clin Endocrinol Metab.* 2012;97(10):3807-3814.